



HAL
open science

Basal ganglia beta oscillations during sleep underlie Parkinsonian insomnia

Aviv Mizrahi-Kliger, Alexander Kaplan, Zvi Israel, Marc Deffains, Hagai
Bergman

► **To cite this version:**

Aviv Mizrahi-Kliger, Alexander Kaplan, Zvi Israel, Marc Deffains, Hagai Bergman. Basal ganglia beta oscillations during sleep underlie Parkinsonian insomnia. *Proceedings of the National Academy of Sciences of the United States of America*, 2020, 117 (29), pp.17359-17368. 10.1073/pnas.2001560117 . hal-03838668

HAL Id: hal-03838668

<https://hal.science/hal-03838668v1>

Submitted on 9 Nov 2022

HAL is a multi-disciplinary open access archive for the deposit and dissemination of scientific research documents, whether they are published or not. The documents may come from teaching and research institutions in France or abroad, or from public or private research centers.

L'archive ouverte pluridisciplinaire **HAL**, est destinée au dépôt et à la diffusion de documents scientifiques de niveau recherche, publiés ou non, émanant des établissements d'enseignement et de recherche français ou étrangers, des laboratoires publics ou privés.

22 Abstract

23 Sleep disorders are among the most debilitating comorbidities of Parkinson's disease
24 (PD) and affect the majority of patients. Of these, the most common is insomnia, the
25 difficulty to initiate and maintain sleep. The degree of insomnia correlates with PD
26 severity and it responds to treatments that decrease pathological basal ganglia (BG)
27 beta oscillations (10-17 Hz in primates), suggesting that beta activity in the BG may
28 contribute to insomnia. We used multiple electrodes to record BG spiking and field
29 potentials during normal sleep and in MPTP-induced Parkinsonism in non-human
30 primates. MPTP intoxication resulted in severe insomnia with delayed sleep onset,
31 sleep fragmentation and increased wakefulness. Insomnia was accompanied by the
32 onset of non-rapid eye movement (NREM) sleep beta oscillations that were
33 synchronized across the BG and cerebral cortex. The BG beta oscillatory activity was
34 associated with a decrease in slow oscillations (0.1-2 Hz) throughout the cortex, and
35 spontaneous awakenings were preceded by an increase in BG beta activity and cortico-
36 BG beta coherence. Finally, the increase in beta oscillations in the basal ganglia during
37 sleep paralleled decreased NREM sleep, increased wakefulness and more frequent
38 awakenings. These results identify NREM sleep beta oscillation in the BG as a neural
39 correlate of PD insomnia and suggest a mechanism by which this disorder could
40 emerge.

41 **Keywords:** Sleep, Parkinson's disease, Insomnia, Beta oscillations

42

43 Significance statement

44 Basal ganglia (BG) beta oscillations are a hallmark of Parkinson's disease (PD), and
45 are specifically reported to correlate with akinesia and rigidity during wakefulness.
46 Studying spontaneous sleep in the non-human primate MPTP model of PD, we report

47 that beta oscillations persist into NREM sleep. In the setting of the sleeping brain, BG
48 beta oscillations correlate with a reduction of slow oscillations across the cortex and
49 BG, and scale with insomnia severity. We suggest that similarly to the way
50 synchronous cortico-BG beta oscillations are postulated to advance the PD akinetic
51 motor symptoms during wakefulness, they may contribute to slow oscillation de-
52 stabilization and insomnia during sleep, thereby underlying two seemingly diverging
53 symptoms of PD.

54 Introduction

55 Parkinson's disease (PD) patients suffer from a myriad of non-motor symptoms
56 including severe sleep disorders (1–4). Insomnia, the difficulty to initiate and maintain
57 sleep (1, 5), affects as many as 60% of all PD patients (5, 6). Among its many long-
58 term consequences, insomnia increases the risk of cognitive decline (7) and mental
59 illness (8, 9), and is a significant predictor of poor quality of life (10). Several
60 mechanisms have been proposed to account for insomnia in PD, including the
61 degeneration of brainstem or hypothalamic nuclei governing sleep (11, 12), the
62 persistence of motor symptoms during sleep (5), the medical therapy (3, 4) and even
63 some comorbid situations, such as depression, restless leg syndrome, and autonomic
64 symptoms (e.g., urinary and gastrointestinal dysfunction) (3, 13, 14). Nonetheless,
65 data relating insomnia in PD (or in the MPTP-intoxicated primate, its leading animal
66 model) to specific alterations in neuronal activity are not available to date.

67 Beta oscillations were recorded in the normal brain (15, 16), but they are especially
68 prominent in the basal ganglia (BG) in idiopathic PD (17) and its animal models (18),
69 where they were postulated to represent aberrant information processing in the BG
70 main axis (19). The beta frequency band varies across species. In MPTP-intoxicated
71 primates it overlaps the low beta band seen in PD patients and spans the 10-17 Hz
72 range (20). Beta oscillations are commonly found during wakefulness and are
73 correlated with awake PD motor symptoms (21), but were also recently observed in
74 BG field potentials during sleep in patients (22–24). However, these findings were
75 heterogeneous across individuals, did not extend to BG spiking activity, were limited
76 to the subthalamic nucleus, and notably were not correlated with the severity and the
77 temporal structure of the PD sleep symptoms.

78 The degree of insomnia correlates with PD severity (25) and the sleep symptoms
79 respond to treatments for PD that decrease BG beta activity and ameliorate waking
80 motor symptoms such as dopamine replacement therapy (26) and deep brain
81 stimulation (DBS) (27, 28). This suggests that BG pathophysiological processes may
82 not only play a mediating role in Parkinson's motor symptoms during wakefulness, but
83 also contribute to PD insomnia.

84 Here, we used the non-human primate MPTP (1-methyl-4-phenyl-1,2,3,6-
85 tetrahydropyridine) model of PD (29), which has been shown to replicate the major
86 biochemical, pathological and clinical signs of PD. We conducted whole-night multi-
87 site field potential (FP) and spiking activity recordings from BG structures along with
88 full polysomnography in healthy and Parkinsonian animals, to elucidate the neural
89 underpinnings of PD insomnia.

90

91 Results

92 **Experimental Parkinsonism is associated with severe insomnia**

93 Following a normal sleep recording period two Vervet monkeys were treated with
94 systemic injections of the neurotoxin MPTP, which rendered them severely
95 Parkinsonian. The neuronal recordings targeted the subthalamic nucleus (STN) and the
96 globus pallidus, external (GPe) and internal (GPi) segments, representing three
97 computational hubs of the BG in which alterations in neuronal activity have been
98 detected in PD during wakefulness (30). The recordings followed the normal
99 light/dark and sleep schedules of the monkeys, lasted throughout the night, and were
100 assisted by full polysomnography (electroencephalogram [EEG], electrooculogram
101 [EOG] and electromyogram [EMG]) and video recordings. The MPTP-intoxicated

102 monkeys were treated with L-DOPA/carbidopa in the morning. Sleep recordings were
103 carried out at least 12 hours after the last L-DOPA dose (OFF stage).

104 After the MPTP treatment, the animals exhibited the motor symptoms characteristic of
105 PD, including bradykinesia, tremor, rigidity and a flexed posture during the day (Fig.
106 1A). The Parkinsonian state was accompanied by severe insomnia, as was previously
107 shown for PD (1, 3) and its MPTP macaque model (31, 32). Representative
108 hypnograms for the normal and MPTP states are provided in Fig. 1B-C. Parkinsonian
109 nights were characterized by a decrease in NREM sleep (including N1/2 and deeper
110 slow wave sleep, SWS) and an increase in wakefulness and transitional states (Fig. 1D
111 and SI appendix, Fig. S1). MPTP intoxication resulted in an elongation of the time
112 needed for the monkeys to fall asleep (from an average of 3.52 minutes to 15.39
113 minutes, Fig. 1E), and in a decrease in consolidated NREM sleep (Fig. 1F. A
114 consolidated bout of NREM sleep was defined as an uninterrupted stretch of NREM
115 sleep lasting 40 seconds or more, see SI appendix. Consolidated SWS also showed a
116 decrease: Normal vs. MPTP, 9.81% vs. 0.99% of all classified epochs, $P = 3.92 \times 10^{-9}$,
117 Mann-Whitney U test). Sleep was not only diminished and harder to initiate, but was
118 also fragmented: the monkeys failed to maintain long sleeping bouts, waking up every
119 ~3.5 minutes on average (vs. every ~13.5 minutes during normal sleep, Fig. 1G) and
120 experiencing longer waking bouts during the night (Fig. 1H). To arrive at a unified
121 measure of the degree of insomnia that incorporated the extended time to sleep onset,
122 decreased consolidated NREM sleep, increased frequency of awakenings and
123 protracted waking time after sleep onset, we defined the sleep quality score (ranging
124 from 0, considerable insomnia, to 1, relatively stable sleep, see Methods). MPTP
125 intoxication significantly reduced the sleep quality score (0.88 before vs. 0.45 after,
126 Fig. 1I-J). Sleep quality improved over recording days, but never reached pre-MPTP

127 intoxication levels (Fig. 1I). As previously reported for macaque monkeys and cats
128 (31–33), REM sleep was completely abolished for five recording nights after
129 intoxication for monkey 1 and two nights for monkey 2, but then partially recovered.
130 Here we concentrate on the effects of induced Parkinsonism on NREM sleep.

131

132 **Insomnia is accompanied by the onset of BG and cortical beta oscillations during**
133 **NREM sleep**

134 We previously reported (34) that during NREM sleep in the normal monkey, BG
135 neurons maintain a state of high amplitude slow oscillatory activity (0.1-2 Hz, Fig. 2A,
136 Fig. 5A, dark traces). In contrast, Parkinsonian NREM sleep was characterized by
137 aberrant beta (10-17 Hz) oscillations throughout the BG, in both the FP and multi-unit
138 spiking levels (Fig. 2C-D, and see the example in Fig. 2B). Power spectral analysis of
139 all FP recording sites in each BG structure revealed that beta activity was more
140 prominent during Parkinsonian sleep than in normal sleep (Fig. 2C), and that a more
141 substantial fraction of FP recording sites during NREM sleep in the Parkinsonian
142 monkey showed beta activity (Fig. 2C, inset). As with the FP, beta oscillations were
143 more prominent and prevalent in BG neuronal multi-unit spiking during NREM sleep
144 in the MPTP vs. the healthy monkey (Fig. 2D). Accordingly, FP and spiking beta
145 power was higher during NREM sleep in the MPTP monkey than in the normal
146 monkey (Fig. 2E-F).

147 The emergence of beta activity in the BG was also manifested in the increase in beta
148 episodes (18, 35) during Parkinsonian NREM sleep. For the field potential as well as
149 the spiking activity, MPTP intoxication increased the probability of beta episodes; i.e.,
150 the total duration of beta episodes in a sleep epoch out of the full epoch length (Fig.
151 2G-H). This was a result of longer episode duration (Fig. 2G-H, upper inset) and

152 increased episode frequency (Fig. 2G-H, lower inset) during NREM sleep post-MPTP
153 intoxication, relative to the normal monkey. These findings are consistent with results
154 acquired from awake PD patients (35) and monkeys (18).

155 Basal ganglia beta activity is widely reported in awake PD patients (19) and MPTP
156 monkeys (18). In our data, BG beta power in the awake monkey was significantly
157 higher than during NREM sleep for FP activity in the GPi and for spiking activity in
158 the GPi and STN (Fig. 2E-F). Similarly, the probability of FP beta episodes was
159 higher during wakefulness in the GPi (9.89% during NREM sleep vs. 15.85% during
160 wakefulness, $P = 1.16 \times 10^{-5}$, Mann-Whitney U test). Thus, even if elevated during
161 wakefulness, beta activity is prevalent in the BG over the entire vigilance cycle, and in
162 the GPe it is as prominent during NREM sleep as it is during wakefulness.

163 Beta oscillations were not confined to the basal ganglia but were also recorded in the
164 cerebral cortex (See example in Fig. 3A). They were evident in the scalp EEG during
165 Parkinsonian NREM sleep (Fig. 3B-C, light traces and boxplots) but not during
166 normal sleep (Fig. 3B-C, dark traces and boxplots). After MPTP intoxication EEG
167 beta power was as prominent during NREM sleep as it was during wakefulness (Fig.
168 3B-C), indicating that cortical beta activity during Parkinsonian sleep may be as
169 clinically significant as it is during wakefulness. Finally, EEG beta episodes during
170 Parkinsonian sleep displayed a similar profile to those in the BG, being more probable,
171 more frequent and lasting longer than beta episodes during normal sleep (Fig. 3D).

172

173 **Beta oscillations are coherent across the BG and cortex**

174 During normal wakefulness, BG spiking activity maintains a state of decorrelated
175 firing (36). BG slow oscillations in firing rate (0.1-2 Hz) remain desynchronized even
176 during normal SWS, one of the most synchronized brain states (34), and during

177 Parkinsonian NREM sleep (SI appendix, Fig. S2). We examined whether this defining
178 feature of normal BG physiology would persist in Parkinsonian sleep beta activity,
179 given the robust emergence of synchronous beta oscillations in awake Parkinsonian
180 animals (18). To that end, we simultaneously recorded FP and spiking activity in the
181 BG using 2-4 microelectrodes (located 0.5-2 mm apart). Fig. 4 provides an example of
182 a two-electrode recording exhibiting synchronous beta activity in the GPi FP (Fig. 4A)
183 and spiking (Fig. 4B). At the population level, beta oscillations in both FP (Fig. 4C)
184 and spiking (Fig. 4D) were coherent between recording sites within BG nuclei.
185 Further, the BG also displayed increased FP-spiking coherence in the beta range (Fig.
186 4E).

187 BG beta oscillations were not only coherent within the BG, but also between EEG
188 contacts (Fig. 4F) and between EEG and simultaneously recorded BG FP (Fig. 4G)
189 and spiking (Fig. 4H) beta oscillations. Finally, FP and EEG beta coherence during
190 normal sleep were similar to the MPTP monkey. This was not true for spiking and FP-
191 spiking beta coherence, which were negligible in the normal monkey (SI appendix,
192 Fig. S3).

193

194 **The increase in BG beta activity during NREM sleep is correlated with a**
195 **decrease in slow oscillations**

196 The increase in beta activity during NREM sleep in the Parkinsonian monkey, in
197 comparison with the normal monkey, coincided with a decrease in GPe and GPi firing
198 rate slow oscillations (SOs, Fig. 5A-B). We analyzed the firing rate power spectra
199 (which is based on the firing rate activity extracted from detected single-neuron action
200 potentials) since SOs in firing rate have been shown to characterize normal NREM
201 sleep (34). The firing rate power spectra should not be confused with multi-unit

202 spiking power spectra, that are based on the electric fields of multiple neurons around
203 the electrode, and were shown in Fig. 2 to exhibit increased beta activity (see
204 Methods). Note that unlike the GPe and GPi, SO showed a tendency to increase in the
205 MPTP monkeys in the STN. A decrease in NREM sleep SOs in the Parkinsonian
206 monkey was also evident in the scalp EEG (Fig. 3A, 5C-D).

207 To determine whether the breakdown of slow oscillations and the onset of beta activity
208 were related, we correlated the SO power changes in the EEG and BG firing rate with
209 concurrent BG FP and spiking beta power. Changes in beta oscillation and slow
210 oscillation were correlated: as field potential and spiking beta power increased, firing
211 rate SO power decreased (Fig. 5E-F). Similarly, the correlation between BG beta
212 power and concurrent cortical EEG SO power (ipsilateral frontal, central and occipital
213 locations) during Parkinsonian NREM sleep was negative (Fig. 5G, I). This correlation
214 ranged from -0.27 to -0.39 for the FP, and from -0.33 to -0.40 for the spiking activity
215 (Fig. 5H, J). Fig. 5H and 5J display only those sites for which the correlation was
216 significant. For the FP, these constituted the majority of cases, whereas for the spiking
217 activity significant correlations were found in fewer than half the sites. Importantly,
218 for both FP and spiking, all of these significant correlations were negative (except for
219 a single FP STN site).

220

221 **BG beta activity rises before spontaneous awakening and is associated with**
222 **diminished and fragmented sleep**

223 If slow oscillation power could be taken to reflect NREM sleep depth (37, 38), then it
224 is possible that the implication of the correlation between increased beta oscillations
225 and decreased slow oscillations could extend to overall changes in sleep architecture
226 (Fig. 1). We examined whether the measures of FP and spiking beta activity reported

227 thus far would vary with the vigilance cycle, and specifically how these changes might
228 relate to periods of lighter NREM sleep (e.g., falling asleep and awakening) and
229 deeper sleep (SWS). Analysis of the dynamics of FP beta power, beta episode
230 probability and FP-EEG beta coherence in all BG nodes during NREM sleep revealed
231 that falling asleep (i.e. uninterrupted NREM sleep following an initial waking state)
232 was associated with a gradual decrease in the FP beta activity across the BG (Fig. 6A-
233 B). Slow wave sleep was associated with relatively minimal FP beta power and beta
234 episode probability, and beta oscillations became more prominent towards wake-up.
235 Similar dynamics were exhibited by the BG FP to EEG beta coherence that decreased
236 as sleep deepened and increased prior to awakening (Fig. 6C). Spiking beta power and
237 probability displayed similar trends, in that they decreased as NREM sleep deepened
238 and were greater post-awakening relative to SWS. However, these trends reached
239 statistical significance only for some BG nodes and were weaker than for the FP.

240 We examined whether the negative correlation between BG beta and cortico-BG SO
241 activity during sleep (Fig. 5) was also reflected in SO power dynamics. EEG SO
242 power increased from NREM sleep onset to culminate during SWS, and remained
243 relatively unchanged until awakening, after which it decreased sharply (Fig. 6D).
244 STN and GPe firing rate SO power exhibited similar behavior: SO power during deep
245 stages of NREM sleep was significantly increased relative to SO power during
246 wakefulness and during NREM sleep immediately after falling asleep (SI appendix,
247 Fig. S4).

248 Next, we examined whether NREM sleep beta oscillation power in the BG was
249 correlated with the overall degree of insomnia. For each NREM sleep epoch, we
250 averaged the beta power across all simultaneously recorded FP or spiking traces in all
251 recording sites in a given BG nucleus. We parceled each night into overlapping

252 periods covering 25% of the total night length (see Methods), and then calculated the
253 fraction of NREM sleep and wakefulness (out of the total duration of staged epochs),
254 and the frequency of awakenings for each segment. Next, for each such period, the
255 average per-structure NREM sleep beta power was calculated. Finally, all the
256 recording periods from a single night were assigned to six groups based on the NREM
257 sleep beta power they exhibited, relative to the total range of beta power that night (the
258 first group had the lowest average beta, and the sixth group had the highest).

259 Analysis of the relationship between the average FP/spiking beta power and the
260 polysomnographic measures across nights showed that for the Parkinsonian monkey,
261 periods with higher average NREM sleep beta power across the BG were
262 characterized by decreased NREM sleep propensity, increased waking propensity and
263 elevated awakening frequency (Fig. 6E for FP and Fig. 6F for spiking, solid light
264 traces). Thus, an increase in beta oscillation in the Parkinsonian monkey was
265 associated with a decrease in slow oscillations at the single-second level, preceded
266 spontaneous awakenings at the level of single sleep bouts, and correlated with more
267 profound insomnia at the level of the entire sleep cycle.

268 Finally, muscle rigidity has been hypothesized to contribute to sleep symptoms in PD
269 (5). To study the possible contribution of rigidity to insomnia, we used trapezius tone
270 (quantified as the root mean square of the EMG signal) as a marker for muscle rigidity
271 (39). We found an increase in trapezius tone in the Parkinsonian monkey (SI appendix,
272 Fig. S5A), but failed to detect a correlation between the trapezius tone and EEG beta
273 activity (SI appendix, Fig. S5B) or FP beta activity in the GPe, GPi or STN (SI
274 appendix, Fig. S5C-E) during NREM sleep. There was no association between
275 increased trapezius tone and decreased NREM sleep, increased wakefulness or
276 increased awakening frequency (SI appendix, Fig. S5F-H).

277

278 Discussion

279 **BG beta oscillations are elevated during Parkinsonian sleep**

280 Beta oscillations have been studied in the healthy brain, where they were suggested to
281 represent a "status quo" state of the motor system (15) or to play a role in working
282 memory (16). However, beta oscillatory activity is particularly prominent in the BG of
283 patients with idiopathic Parkinson's disease (PD) (19), where it correlates primarily
284 with akinesia and rigidity during wakefulness (21). Further, the extent of clinical
285 benefit in akinesia and rigidity is correlated with the decrease in FP beta power in PD
286 patients (40). In our MPTP model beta activity was consistently more prominent and
287 widespread in the Parkinsonian monkey, also during NREM sleep. The Parkinsonian
288 state was also accompanied by an increase in beta coherence within the BG and cortex,
289 and between them. One finding that challenged this rule was relatively elevated FP
290 and EEG beta coherence during normal sleep. This elevated coherence may be due to
291 volume conductance of lower amplitude beta activity in the cortex and BG, which
292 does not pertain to unit spiking.

293 Beta oscillations during sleep were reported in three studies that used FP data obtained
294 from the STN of human PD patients. All showed beta during NREM sleep (22–24),
295 but neither showed any relationship between beta oscillations and the severity or
296 temporal structure of sleep disorders. Here, we introduce beta oscillation as a neural
297 correlate for PD insomnia and report the relationship between beta activity and NREM
298 sleep quality in Parkinsonism.

299

300 **The differences between MPTP insomnia and PD insomnia**

301 The above human studies reported modest NREM sleep beta activity in the STN,
302 relative to wakefulness (22–24). In our results beta activity was prominent during
303 NREM sleep, and for some cases, like the scalp EEG, it was comparable to waking
304 beta. This difference in NREM sleep beta activity may reflect the fact that MPTP does
305 not fully capture the natural history and clinical manifestation of idiopathic PD. Our
306 MPTP paradigm introduces a more fulminant and more severe disability than that
307 found in PD patients undergoing STN DBS surgery. Furthermore, the acuteness of
308 MPTP intoxication raises the concern that its effect might subside over time, thereby
309 not replicating the sleep impairments seen in PD. In our model, beta activity and its
310 relationship with the vigilance cycle were stable across 26 recording days, apart from a
311 decrease in GPe FP beta power to above-normal levels in the last few recording days.
312 Sleep quality improved in the last days of recording, but stayed significantly lower
313 than pre-intoxication levels. Possible contributing factors to this improvement might
314 be partial resolution of the MPTP effect on the dopaminergic system or on other
315 neuro-modulatory system over time (41) and our chronic administration of L-DOPA
316 that might have had long-term effects (42).

317 Concerning the molecular mechanisms eliciting insomnia in our model and in
318 idiopathic PD, we cannot rule out the possibility that MPTP insomnia is caused by a
319 different mechanism than PD insomnia. Our use of MPTP may have resulted in toxic
320 injury to other brain structures orchestrating sleep (43) or the circadian rhythm (44)
321 that are not severely affected in idiopathic PD. Inversely, PD insomnia might be
322 mediated by the degeneration of cell groups that are spared by MPTP intoxication,
323 such as the orexin neurons (45). However, the similarity between the sleep disorders
324 reported here and in other works using MPTP monkeys (31, 32), and the sleep
325 disorders in idiopathic PD (5), does suggest that the process mediating insomnia may

326 be common to PD and MPTP intoxication (i.e., the degeneration of substantia nigra
327 pars compacta dopaminergic neurons (14) and other brain monoaminergic neurons).
328 Further, the fact that the sleep symptoms in the idiopathic disease respond to
329 treatments that decrease BG beta activity (26–28) offers support to the hypothesis that
330 the pathophysiological pathways for PD insomnia and MPTP insomnia are at least
331 partially overlapping.

332

333 **Beta oscillations are different than sleep spindles**

334 An overlap exists between the frequency ranges of beta oscillations and sleep spindles
335 that are prevalent in normal NREM sleep (46, 47). It is possible that normal or
336 pathological sleep spindle activity was detected by our methods as beta activity.
337 However, beta activity in our data exhibited two features that do not classically
338 characterize sleep spindles. First, both normal and Parkinsonian beta episodes had
339 significantly shorter durations and higher frequencies of occurrence compared to
340 cortical sleep spindles in primates (Fig. 2G, H and 3D) (47). Second, BG and cortical
341 beta oscillations in the Parkinsonian monkey were similarly prevalent during sleep and
342 during wakefulness. In contrast, in the normal monkey they were relatively weak
343 regardless of the vigilance cycle (Fig. 2E, F and 3B, C). This would not be expected
344 from sleep spindles, a hallmark of NREM sleep (46).

345

346 **Cortico-BG beta oscillations may contribute to insomnia in Parkinsonism**

347 Although the mechanism of beta generation and propagation through the cortex and
348 BG in Parkinsonism is still debated (48), evidence shows that the BG are an important
349 hub for the generation of beta oscillations (49). Waking BG beta oscillatory output is
350 hypothesized to disrupt cortical computation in PD (17), possibly contributing to the

351 waking symptoms of the disease (50). The BG output structures (GPi and substantia
352 nigra pars reticulata, SNr) target a number of thalamic nuclei that innervate the frontal
353 cortex where slow oscillations emerge during sleep (38). Thus, similar to wakefulness,
354 synchronized beta oscillations from the BG could be transmitted to cortical areas,
355 disrupting the generation or propagation of cortical slow oscillations during NREM
356 sleep and contributing to insomnia. This putative mechanism is congruent with the
357 observation that increased BG beta power is associated with a decrease in cortical slow
358 oscillation (Fig. 5G-J), that beta activity increases prior to awakening (Fig. 6A-C) and
359 correlates with the severity of insomnia (Fig. 6E, F) and that SO power falls upon
360 awakening (Fig. 6D). Remarkably, STN DBS, which has been shown to reduce beta
361 oscillation (51), is associated with an improvement in subjective sleep quality (27) and
362 reductions in insomnia and sleep fragmentation in PD (27, 28). Finally, a dual BG
363 involvement in sleep homeostasis and motor control was recently supported by a work
364 showing that GAD2 neurons in the SNr promote sleep generation, possibly through
365 their projections to various monoaminergic nuclei orchestrating the vigilance cycle
366 (52).

367

368 **Additional possible factors contributing to PD insomnia**

369 Although this work provides strong correlational links between beta oscillations and
370 insomnia in Parkinsonism, this correlation does not imply causation. Insomnia in
371 idiopathic PD may result from a host of other factors such as an underlying
372 neurodegenerative process affecting brainstem or hypothalamic sleep/wake centers
373 (11, 12), PD medical treatment (3, 4) or comorbid situations including depression (13),
374 restless leg syndrome and nocturia (14). Even if insomnia does originate from a BG
375 pathology subsequent to dopaminergic denervation, it might not be a direct

376 consequence of beta oscillation. Rather, it could result from PD motor symptoms (5)
377 such as muscle rigidity. This setting, where beta oscillations might only serve as a
378 surrogate marker for disease severity, could possibly be reflected in the correlation
379 found here between the degree of insomnia and beta power. However, in our data,
380 there was no association between muscle rigidity and beta activity in the EEG or in the
381 BG, or between muscle rigidity and sleep quality. Additionally, in a study that
382 assessed the effect of nocturnal DBS on PD patients, the number of body position
383 changes during sleep was similar before and on stimulation (27). These findings
384 suggest that insomnia in our model, and generally in PD, cannot be attributed solely to
385 the persistence of motor symptoms into sleep.

386

387 **Conclusions**

388 In the MPTP-treated Parkinsonian monkey, NREM sleep beta oscillations were
389 associated with reduced cortical slow oscillations, increased before spontaneous
390 awakening and correlated with the degree of insomnia. Thus, beta oscillations may be
391 used as a marker for both the waking motor and sleep-related symptoms of PD. Phase-
392 specific brain stimulation was recently shown to either augment or suppress brain
393 oscillations (53, 54). Thus, future closed-loop adaptive DBS therapy for PD aimed at
394 suppressing NREM beta oscillations and augmenting slow oscillations by phase
395 specific stimulation could be helpful in the control of insomnia in PD.

396 Methods

397 All experimental protocols were conducted in accordance with the National Institute of
398 Health Guide for Care and Use of Laboratory Animals and with the Hebrew
399 University guidelines for the use and care of laboratory animals in research. The
400 experiments were supervised by the institutional Animal Care and Use Committee of
401 the Faculty of Medicine, the Hebrew University. The Hebrew University is an
402 internationally accredited institute of the Association for Assessment and
403 Accreditation of Laboratory Animal Care (AAALAC).

404 The following subsections are to be found in the SI appendix Methods section:
405 Animals, sleep habituation and surgery; MPTP intoxication; Polysomnography and
406 sleep staging; Electrophysiological Recordings and Data Collection; Synchronization
407 analysis; Beta episode analysis; Coherence analysis and EMG tone analysis.

408

409 **Analysis of sleep measures**

410 For each recording night a number of sleep architecture measures were obtained. Sleep
411 onset was defined as the start of the first bout of at least 40 seconds that the monkey
412 spent in NREM or REM sleep. The time to sleep onset was defined as the time elapsed
413 since the monkey was left in the dark recording chamber to sleep onset. Wakefulness
414 after sleep onset (WASO) was calculated as the total waking time after sleep onset,
415 divided by the total length of all classified epochs. A bout of consolidated NREM
416 sleep/SWS was defined as a stretch of at least 40 seconds of NREM sleep/SWS.
417 Finally, the frequency of awakenings per hour was calculated as the number of
418 transitions from any sleep stage to a period of wakefulness lasting at least 30 seconds,
419 throughout the night, divided by the total recording time in hours. Using various
420 higher and lower duration thresholds provided similar results.

421 For each night, each aforementioned sleep measure was normalized to the 0 to 1 range
422 by dividing by the range delineated by the minimal and maximal value of the sleep
423 measure across all normal and MPTP nights (after subtraction of the minimal value).

424 Then, the sleep quality score for that night was obtained in the following manner:

$$425 \quad \textit{Sleep Quality Score} = (\textit{normalized consolidated NREM sleep} + 1 - \textit{normalized time to} \\ 426 \quad \textit{sleep onset} + 1 - \textit{normalized awakening frequency} + 1 - \textit{normalized WASO})/4$$

427 The sleep quality score ranged from 0 to 1, increasing as NREM sleep became more
428 abundant and as the time to sleep onset, awakening frequency and WASO decreased.

429

430 **Power spectrum analysis**

431 Each neuronal unit's recording time was divided into 10-second epochs corresponding
432 to the sleep staging epochs. We conducted a spectral analysis of the FP and the spiking
433 activity recorded in the vicinity of each of the analyzed neurons. The raw signal
434 (hardware filtration, 0.075 Hz-10 kHz, sampling at 44 kHz) was digitally bandpass
435 filtered using a zero-phase Butterworth filter (0.1-300 Hz, bandstop at 0.05 and 350
436 Hz for FP; 300-6,000 Hz, bandstop at 200 and 6,500 Hz for spiking) and down-
437 sampled to 1,375 samples/s (FP) or to 11,000 samples/s (spiking). Spiking traces were
438 further full-wave rectified, and all the real-time detected (high-amplitude) spikes,
439 which represent the firing of a single proximal neuron, were removed to obtain a less
440 biased representation of the multi-unit signal. Spike removal was done by automated
441 detection and replacement of spike waveforms with white noise generated as a random
442 vector of numbers with a mean identical to the 10-second epoch average voltage and a
443 range between one-half a standard deviation (of the entire voltage trace from which
444 spikes were removed) below and above the mean. In roughly one third of the recording
445 sites, across BG structures and recording days, a high-power, narrow band peak

446 (mostly 0.34 Hz at its base) appeared at ~17.5 Hz in the FP spectrum. Due to the
447 extremely narrow frequency band characterizing it and its resemblance to higher
448 frequency artifactual peaks (i.e., at 50 Hz), these recordings were filtered with a
449 narrow band Butterworth notch filter prior to further analysis. FP and spiking signals,
450 post filtration, were converted to z-scores.

451 Power spectra for both FP and spiking signals were obtained using 16,384 (FP) or
452 131,072 (spiking) FFT point Hamming windows, yielding a frequency resolution of
453 0.084 Hz. The relative power at each frequency was then calculated by division of the
454 entire spectrum by the overall power in the range of 0.1-40 Hz.

455 For each FP/spiking recording site, beta power was calculated in relation to the power
456 in two adjacent frequency ranges. First, a 5-point Gaussian kernel was used to smooth
457 the average power spectrum. Next, a beta peak was detected in the 11-15 Hz range,
458 and the average power 3 Hz around it was calculated. The choice of the 11-15 Hz
459 range was motivated by the observation that in the vast majority of cells, pathological
460 beta power was concentrated within these bounds. Further, it guaranteed that the 3-Hz
461 segment around the peak would be within the 10-17 Hz range. The power in the left
462 flanking frequency range was the average power 2 Hz around a similarly detected
463 trough in the 6-10 Hz range, and the power in the right flanking frequency range was
464 set to be the average power at 20-25 Hz. Beta power was calculated as the average
465 power around the beta peak minus the average power across both flanks (SI appendix,
466 Fig. S6). A spiking/FP location was considered as exhibiting beta activity if its beta
467 power exceeded a predefined threshold (different for spiking and FP, constant across
468 structures and between normal and MPTP data).

469 In addition, for each recorded neuron we calculated the firing rate power spectrum: for
470 each 10-second epoch, a firing rate vector was calculated based on the detected action

471 potentials from that neuron, in 5-ms non-overlapping bins. The per-epoch firing rate
472 power spectrum was obtained from the firing rate signal.

473

474 **Beta to slow oscillation correlation analysis**

475 For the analysis of beta and slow oscillations during NREM sleep in the FP/spiking
476 and EEG signals, all signals were filtered and normalized as described above. The only
477 exception was for the power spectrum normalization of the EEG power, in which slow
478 oscillations were detected. Instead of being normalized by division by total power, it
479 was divided by the total power excluding the beta range. This was done to make sure
480 that no artifactual negative correlations were detected due to the increase in EEG beta
481 power that was concurrent with the increase in FP/spiking beta power. The correlation
482 between BG and cortical activity was only calculated for BG sites (FP/spiking) that
483 exhibited beta oscillations. For each site, the correlation coefficient between EEG
484 beta/SO and BG beta was calculated over all 10-second epochs in which FP/spiking
485 activity was recorded from that site. The results were similar across various other
486 normalization methods. The analyses reported in Fig. 3-6 returned similar results when
487 performed separately for each of the different EEG derivations examined. Therefore,
488 data from the different EEG derivations are averaged in these figures.

489

490 **BG beta power and polysomnographic events**

491 To arrive at a measure of the average FP NREM sleep beta power across BG recording
492 sites, the power in the beta range was first calculated for each NREM epoch in each FP
493 recording site, as explained above. Next, the per-BG structure average beta power was
494 calculated across all simultaneously recorded FP traces in the GPe, GPi or STN. The
495 night was divided into overlapping periods lasting 25% of the total night length (100

496 seconds separating the onsets of two consecutive periods). The average NREM sleep
497 BG beta power, as well as the percentage of NREM sleep and wakefulness, and the
498 hourly awakening frequency, were calculated for each period. We chose to parcel the
499 night into relatively long periods to increase the accuracy of the polysomnographic
500 measure estimation. The use of overlapping periods allowed us to detect finer
501 modulations of beta activity throughout the night. The analysis of longer and shorter
502 period lengths resulted in similar results. Finally, all the recording periods obtained in
503 a single night were assigned to six groups based on the NREM sleep beta power they
504 exhibited, relative to the total range of beta power that night (the first group had the
505 lowest average beta power and the sixth group had the highest). For each group, the
506 average of the polysomnographic measures was calculated. Data from all nights and
507 structures were pooled.

508 The analysis of spiking activity was identical except that for the FP data, beta power
509 was first averaged across all simultaneously recorded sites and then grouped. For the
510 spiking data, beta power was not averaged across recording sites; rather the grouping
511 was carried out for each recording site individually. The rationale behind this
512 separation was that the FP is a highly correlated signal across the BG (as also shown in
513 Fig. 4), whereas different cells could exhibit different levels of basal spiking beta
514 power. A relatively higher spiking beta power for one recording location could be
515 similar to a lower spiking beta power for a different location, and averaging these
516 different levels together could potentially cancel out trends that would have been
517 meaningful at the single spiking trace level. Thus, for spiking activity, the data were
518 first assigned to beta power groups at the individual spiking trace level and only then
519 averaged over all simultaneously recorded sites.

520

521 **Statistics**

522 Analyses were conducted identically on the different neuronal assemblies. The data
523 from the two monkeys were pooled since no significant differences were detected
524 between them. A threshold of 0.05 was used to establish statistical significance. Non-
525 parametric statistical tests were used throughout this manuscript (The Mann-Whitney
526 U test for two non-paired groups, the Wilcoxon signed rank test for two paired groups,
527 and the Kruskal-Wallis H test for more than two groups). For multiple comparisons,
528 the FDR correction (Benjamini-Hochberg procedure) was utilized. Analyses were
529 performed using Matlab 2013a (Mathworks, MA, USA). Data, code and other
530 materials are available from the Basal Ganglia data repository
531 (basalganglia.huji.ac.il/links.htm).

532

533 Acknowledgments

534 We thank Yaron Dagan and Tamar Ravins-Yaish for assistance with animal care, Atira
535 Bick and Adi Payis for assistance with the MRI scan, Hila Gabbay, Sharon Freeman,
536 Uri Werner-Reiss and Esther Singer for general assistance. We thank Anatoly
537 Shapochnikov for help in preparing the experimental setup. This work was supported
538 by grants from the European Research Council (ERC) and the Rosetrees trust to Hagai
539 Bergman.

540

541 Author contribution

542 A.M.K. and H.B. designed the research, Z.I. performed the surgery, A.M.K., A.K. and
543 M.D. collected the data, A.M.K. analyzed the data, A.M.K., M.D. and H.B. wrote the
544 manuscript. All authors read and commented on the final version of the manuscript.

545 The authors declare no conflict of interest.

546

547

548

549 References

- 550 1. V. C. De Cock, M. Vidailhet, I. Arnulf, Sleep disturbances in patients with
551 parkinsonism. *Nat. Clin. Pract. Neurol.* **4**, 254–266 (2008).
- 552 2. S. A. Factor, T. McAlarney, J. R. Sanchez-Ramos, W. J. Weiner, Sleep
553 disorders and sleep effect in Parkinson’s disease. *Mov. Disord.* **5**, 280–285
554 (1990).
- 555 3. A. Videnovic, B. Högl, *Disorders of Sleep and Circadian Rhythms in*
556 *Parkinson’s Disease*, A. Videnovic, B. Högl, Eds. (Springer Vienna, 2015)
557 <https://doi.org/10.1007/978-3-7091-1631-9>.
- 558 4. L. M. Chahine, A. W. Amara, A. Videnovic, A systematic review of the
559 literature on disorders of sleep and wakefulness in Parkinson’s disease from
560 2005 to 2015. *Sleep Med. Rev.* **35**, 33–50 (2017).
- 561 5. M. Kryger, T. Roth, W. C. Dement, *Principles and Practice of Sleep Medicine*,
562 Elsevier (2017).
- 563 6. M. D. Gjerstad, T. Wentzel-Larsen, D. Aarsland, J. P. Larsen, Insomnia in
564 Parkinson’s disease: frequency and progression over time. *J. Neurol.*
565 *Neurosurg. Psychiatry* **78**, 476–9 (2007).
- 566 7. K. Stavitsky, S. Nearing, Y. Bogdanova, P. McNamara, A. Cronin-Golomb,
567 The Impact of Sleep Quality on Cognitive Functioning in Parkinson’s Disease.
568 *J. Int. Neuropsychol. Soc.* **18**, 108–117 (2012).
- 569 8. K. Suzuki, *et al.*, Correlation between depressive symptoms and nocturnal
570 disturbances in Japanese patients with Parkinson’s disease. *Parkinsonism Relat.*
571 *Disord.* **15**, 15–19 (2009).

- 572 9. S. Rutten, *et al.*, The bidirectional longitudinal relationship between insomnia,
573 depression and anxiety in patients with early-stage, medication-naïve
574 Parkinson's disease. *Parkinsonism Relat. Disord.* **39**, 31–36 (2017).
- 575 10. K. H. Karlsen, J. P. Larsen, E. Tandberg, J. G. Maland, Influence of clinical
576 and demographic variables on quality of life in patients with Parkinson's
577 disease. *J. Neurol. Neurosurg. Psychiatry* **66**, 431–435 (1999).
- 578 11. H. Braak, *et al.*, Staging of brain pathology related to sporadic Parkinson's
579 disease. *Neurobiol. Aging* **24**, 197–211 (2003).
- 580 12. M. E. Kalaitzakis, S. M. Gentleman, R. K. B. Pearce, Disturbed sleep in
581 Parkinson's disease: anatomical and pathological correlates. *Neuropathol.*
582 *Appl. Neurobiol.* **39**, 644–653 (2013).
- 583 13. S. Happe, *et al.*, Sleep disorders and depression in patients with Parkinson's
584 disease. Results of a study with the Sleep Disorders Questionnaire (SDQ) and
585 the Zung Depression Scale (ZDS). *Acta Neurol. Scand.* **104**, 275–280 (2001).
- 586 14. J. M. Monti, S. R. Pandi-Perumal, S. Chokroverty, *Dopamine and Sleep -*
587 *Molecular, Functional, and Clinical Aspects*, J. M. Monti, S. R. Pandi-
588 Perumal, S. Chokroverty, Eds. (Springer Nature, 2016).
- 589 15. A. K. Engel, P. Fries, Beta-band oscillations — signalling the status quo? *Curr.*
590 *Opin. Neurobiol.* **20**, 156–165 (2010).
- 591 16. R. Schmidt, *et al.*, Beta Oscillations in Working Memory, Executive Control of
592 Movement and Thought, and Sensorimotor Function. *J. Neurosci.* **39**, 8231–
593 8238 (2019).

- 594 17. C. Hammond, H. Bergman, P. Brown, Pathological synchronization in
595 Parkinson's disease: networks, models and treatments. *Trends Neurosci.* **30**,
596 357–364 (2007).
- 597 18. M. Deffains, H. Bergman, H. Bergman, Parkinsonism-related β oscillations in
598 the primate basal ganglia networks – Recent advances and clinical
599 implications. *Park. Relat. Disord.* **59**, 2–8 (2019).
- 600 19. P. Brown, Oscillatory nature of human basal ganglia activity: Relationship to
601 the pathophysiology of Parkinson's disease. *Mov. Disord.* **18**, 357–363 (2003).
- 602 20. A. Moran, E. Stein, H. Tischler, I. Bar-Gad, Decoupling neuronal oscillations
603 during subthalamic nucleus stimulation in the parkinsonian primate. *Neurobiol.*
604 *Dis.* **45**, 583–590 (2012).
- 605 21. M. Beudel, *et al.*, Oscillatory Beta Power Correlates With Akinesia-Rigidity in
606 the Parkinsonian Subthalamic Nucleus. *Mov. Disord.* **32**, 174–175 (2017).
- 607 22. E. Urrestarazu, *et al.*, Beta activity in the subthalamic nucleus during sleep in
608 patients with Parkinson's disease. *Mov. Disord.* **24**, 254–260 (2009).
- 609 23. J. A. Thompson, *et al.*, Sleep patterns in Parkinson's disease: direct recordings
610 from the subthalamic nucleus. *J. Neurol. Neurosurg. Psychiatry* **89**, 95–104
611 (2018).
- 612 24. E. Christensen, A. Abosch, J. A. Thompson, J. Zylberberg, Inferring sleep
613 stage from local field potentials recorded in the subthalamic nucleus of
614 Parkinson's patients. *J. Sleep Res.* **28**, e12806 (2019).
- 615 25. M. I. Norlinah, *et al.*, Sleep disturbances in Malaysian patients with

- 616 Parkinson's disease using polysomnography and PDSS. *Parkinsonism Relat.*
617 *Disord.* **15**, 670–674 (2009).
- 618 26. R. Kim, B. Jeon, Nonmotor Effects of Conventional and Transdermal
619 Dopaminergic Therapies in Parkinson's Disease. *Int. Rev. Neurobiol.* **134**, 989–
620 1018 (2017).
- 621 27. H. Baumann-Vogel, *et al.*, The Impact of Subthalamic Deep Brain Stimulation
622 on Sleep–Wake Behavior: A Prospective Electrophysiological Study in 50
623 Parkinson Patients. *Sleep* **40** (2017).
- 624 28. J. R. P. Zuzúárregui, J. L. Ostrem, The Impact of Deep Brain Stimulation on
625 Sleep in Parkinson's Disease: An update. *J. Parkinsons. Dis.* **10**, 393–404
626 (2020).
- 627 29. S. H. Fox, J. M. Brotchie, The MPTP-lesioned non-human primate models of
628 Parkinson's disease. Past, present, and future. *Prog. Brain Res.* **184**, 133–157
629 (2010).
- 630 30. M. Deffains, *et al.*, Subthalamic, not striatal, activity correlates with basal
631 ganglia downstream activity in normal and parkinsonian monkeys. *Elife* **5**, 1–
632 38 (2016).
- 633 31. Q. Barraud, *et al.*, Sleep disorders in Parkinson's disease: The contribution of
634 the MPTP non-human primate model. *Exp. Neurol.* **219**, 574–582 (2009).
- 635 32. H. Belaid, J. Adrien, C. Karachi, E. C. Hirsch, C. François, Effect of melatonin
636 on sleep disorders in a monkey model of Parkinson's disease. *Sleep Med.* **16**,
637 1245–1251 (2015).

- 638 33. K. Pungor, M. Papp, K. Kékesi, G. Juhász, A novel effect of MPTP: the
639 selective suppression of paradoxical sleep in cats. *Brain Res.* **525**, 310–314
640 (1990).
- 641 34. A. D. Mizrahi-Kliger, A. Kaplan, Z. Israel, H. Bergman, Desynchronization of
642 slow oscillations in the basal ganglia during natural sleep. *Proc. Natl. Acad.*
643 *Sci.* **115**, E4274–E4283 (2018).
- 644 35. G. Tinkhauser, *et al.*, The modulatory effect of adaptive deep brain stimulation
645 on beta bursts in Parkinson’s disease. *Brain* **140**, 1053–1067 (2017).
- 646 36. A. Nini, A. Feingold, H. Slovin, H. Bergman, Neurons in the globus pallidus
647 do not show correlated activity in the normal monkey, but phase-locked
648 oscillations appear in the MPTP model of parkinsonism. *J. Neurophysiol.* **74**,
649 1800–1805 (1995).
- 650 37. C. Iber, S. Ancoli-Israel, A. L. Chesson, S. F. Quan, *The AASM Manual for the*
651 *Scoring of Sleep and Associated Events: Rules, Terminology and Technical*
652 *Specifications* (American Association of Sleep Medicine, 2007).
- 653 38. M. Massimini, R. Huber, F. Ferranelli, S. Hill, G. Tononi, The Sleep Slow
654 Oscillation as a Traveling Wave. *J. Neurosci.* **24**, 6862–6870 (2004).
- 655 39. C. Duval, *et al.*, The effect of Trager therapy on the level of evoked stretch
656 responses in patients with Parkinson’s disease and rigidity. *J. Manipulative*
657 *Physiol. Ther.* **25**, 455–464 (2002).
- 658 40. A. A. Kühn, *et al.*, Pathological synchronisation in the subthalamic nucleus of
659 patients with Parkinson’s disease relates to both bradykinesia and rigidity. *Exp.*
660 *Neurol.* **215**, 380–387 (2009).

- 661 41. B. Ballanger, *et al.*, Imaging Dopamine and Serotonin Systems on MPTP
662 Monkeys: A Longitudinal PET Investigation of Compensatory Mechanisms. *J.*
663 *Neurosci.* **36**, 1577–1589 (2016).
- 664 42. H. Belaid, *et al.*, Sleep disorders in Parkinsonian macaques: effects of L-dopa
665 treatment and pedunculopontine nucleus lesion. *J. Neurosci.* **34**, 9124–33
666 (2014).
- 667 43. C. Pifl, G. Schingnitz, O. Hornykiewicz, Effect of 1-methyl-4-phenyl-1,2,3,6-
668 tetrahydropyridine on the regional distribution of brain monoamines in the
669 rhesus monkey. *Neuroscience* **44**, 591–605 (1991).
- 670 44. K. Fifel, *et al.*, Alteration of Daily and Circadian Rhythms following
671 Dopamine Depletion in MPTP Treated Non-Human Primates. *PLoS One* **9**,
672 e86240 (2014).
- 673 45. M. Bensaid, *et al.*, Spraying of orexin-A and orexin-B neurons in the
674 hypothalamus and of orexin fibers in the substantia nigra of 1-methyl-4-phenyl-
675 1,2,3,6-tetrahydropyridine-treated macaques. *Eur. J. Neurosci.* **41**, 129–136
676 (2015).
- 677 46. T. Andrillon, *et al.*, Sleep Spindles in Humans: Insights from Intracranial EEG
678 and Unit Recordings. *J. Neurosci.* **31**, 17821–17834 (2011).
- 679 47. S. Takeuchi, *et al.*, Spatiotemporal Organization and Cross-Frequency
680 Coupling of Sleep Spindles in Primate Cerebral Cortex. *Sleep* **39** (2016).
- 681 48. A. Sharott, *et al.*, Spatio-temporal dynamics of cortical drive to human
682 subthalamic nucleus neurons in Parkinson’s disease. *Neurobiol. Dis.* **112**, 49–
683 62 (2018).

- 684 49. M. D. Bevan, P. J. Magill, D. Terman, J. P. Bolam, C. J. Wilson, Move to the
685 rhythm: oscillations in the subthalamic nucleus–external globus pallidus
686 network. *Trends Neurosci.* **25**, 525–531 (2002).
- 687 50. R. S. Turner, M. Desmurget, Basal ganglia contributions to motor control: a
688 vigorous tutor. *Curr. Opin. Neurobiol.* **20**, 704–716 (2010).
- 689 51. E. J. Quinn, *et al.*, Beta oscillations in freely moving Parkinson’s subjects are
690 attenuated during deep brain stimulation. *Mov. Disord.* **30**, 1750–1758 (2015).
- 691 52. D. Liu, *et al.*, A common hub for sleep and motor control in the substantia
692 nigra. *Science (80-.)*. **367**, 440–445 (2020).
- 693 53. A. B. Holt, *et al.*, Phase-Dependent Suppression of Beta Oscillations in
694 Parkinson’s Disease Patients. *J. Neurosci.* **39**, 1119–1134 (2019).
- 695 54. O. Peles, U. Werner-Reiss, H. Bergman, Z. Israel, E. Vaadia, Phase-Specific
696 Microstimulation Differentially Modulates Beta Oscillations and Affects
697 Behavior. *Cell Rep.* **30**, 2555-2566.e3 (2020).
- 698

699 Figure legends:

700 **Fig. 1** Parkinsonism introduces severe insomnia. (A) Primate PD motor score (range: 0
701 to 12. Bradykinesia, tremor, rigidity and postural deficits were each assigned a score
702 from 0 to 3, where 3 represents severe symptoms) for both monkeys, normal state
703 (mean, 0.00 ± 0.00 , $n = 38$ and $n = 29$ days for monkey 1 and 2, respectively) vs. after
704 MPTP intoxication (monkey 1: mean \pm s.e.m., 6.67 ± 0.13 , $n = 27$ days. Monkey 2:
705 mean, 6.19 ± 0.09 , $n = 18$ days. $P = 2.11 \times 10^{-14}$ and $P = 4.88 \times 10^{-11}$, respectively,
706 Mann-Whitney U test). (B-C) All-night hypnograms for exemplary normal (B) and
707 MPTP (C) nights, monkey 1. (D) Relative proportions of different sleep stages
708 (*unclass.*, unclassified, corresponding to transitional states), out of the total recording
709 time, over all nights and both monkeys. Color scale as in (B) and (C) (Normal
710 monkey, $n = 38$ recording nights for monkey 1 and $n = 29$ for monkey 2. MPTP
711 monkey, $n = 13$ recording nights for monkey 1 and $n = 6$ for monkey 2. Normal vs.
712 MPTP, change in SWS, $P = 6.71 \times 10^{-10}$, N1/2, $P = 0.030$, wakefulness, $P = 8.29 \times 10^{-8}$,
713 REM, $P = 1.50 \times 10^{-4}$, Unclassified, $P = 7.60 \times 10^{-9}$, Mann-Whitney U test). (E) Time to
714 consolidated sleep onset (first sleep bout of length > 40 s), normal vs. MPTP, for both
715 monkeys. $*P < 0.05$, Mann-Whitney U test. Each point represents one night, error bars
716 represent s.e.m., black, monkey 1, gray, monkey 2. A single point in the MPTP bar (at
717 86.17 min) is not included in this plot. (F) Percentage of consolidated NREM sleep out
718 of all classified epochs. normal vs. MPTP. $***P < 0.0001$, Mann-Whitney U test. (G)
719 Awakening frequency, normal vs. MPTP. $***P < 0.0001$, Mann-Whitney U test. (H)
720 Wakefulness after sleep onset (WASO), in % of all classified epochs, normal vs.
721 MPTP. $***P < 0.0001$, Mann-Whitney U test. (I) Sleep quality score for the last
722 normal recording days and MPTP recording days, for both monkeys. Sleep quality
723 improved in the last five recording days relative to the first five days (0.67 vs. 0.37, P

724 = 0.016, but never reached pre-intoxication levels, 0.67 vs. 0.88, $P = 6.67 \times 10^{-4}$, Mann-
725 Whitney U test). (J) Average sleep quality score, normal vs. MPTP, for both monkeys.
726 *** $P < 0.0001$, Mann-Whitney U test. Unless otherwise noted, the data are presented
727 as averages in this and the subsequent figures.

728 **Fig. 2** Parkinsonism is associated with an increase in beta oscillations in the basal
729 ganglia during NREM sleep. (A-B) Typical field potential (FP, top) and concurrent
730 spiking (bottom) recordings from a GPi electrode during NREM sleep in the normal
731 monkey (A) and after MPTP intoxication (B). Horizontal bar, 0.5 s. Vertical bars, 50
732 μ V. Colored are segments of spiking slow oscillation (A, dark blue) and beta
733 oscillation (B, light blue), and their concurrent FP segments. (C) FP power spectra for
734 GPe (red), GPi (blue) and STN (green), during NREM sleep, normal (dark traces) vs.
735 MPTP (light traces). Shading represents s.e.m. Inset, the proportion of FP recording
736 sites exhibiting beta activity, averaged across four different thresholds (see Methods).
737 For the entire figure, n = 305, 172 and 94 sites recorded during NREM sleep (FP and
738 spiking) for the normal GPe, GPi, and STN, respectively (of which n = 161, 61 and 63
739 were obtained from monkey 1, and the rest from monkey 2). n = 211, 51 and 43 for the
740 GPe, GPi, and STN, respectively, during MPTP intoxication (of which n = 154, 15 and
741 20 were obtained from monkey 1, and the rest from monkey 2). (D) Spiking power
742 spectra for GPe, GPi and STN, normal vs. MPTP. Shading and inset as in (C). (E)
743 NREM sleep and wakefulness FP beta power (normalized by subtraction of the
744 average power in the flanking frequency ranges), normal (dark boxplots) vs. MPTP
745 (light boxplots), GPe, GPi and STN, ***P < 0.0001, Mann-Whitney U test. Black line
746 represents the median, boxes represent the 25-75 percentiles and whiskers denote the
747 10 and 90 percentiles. n = 271, 160 and 79 sites recorded during wakefulness (FP and
748 spiking) for the normal GPe, GPi, and STN, respectively (of which n = 129, 50 and 53
749 were obtained from monkey 1, and the rest from monkey 2). n = 209, 50 and 44 for the
750 GPe, GPi, and STN, respectively, during wakefulness following MPTP intoxication
751 (of which n = 152, 13 and 20 were obtained from monkey 1, and the rest from monkey
752 2). For the GPe and STN, MPTP wakefulness vs. NREM, non-significant. (F) NREM

753 sleep and wakefulness spiking beta power, normal vs. MPTP, GPe, GPi and STN, *P
754 < 0.05, ***P < 0.0001, Mann-Whitney U test. For the GPe, MPTP wakefulness vs.
755 NREM, non-significant. (G) NREM sleep FP beta episode probability, beta episode
756 duration (upper inset) and beta episode frequency (lower inset), normal vs. MPTP,
757 GPe, GPi and STN, ***P < 0.0001, Mann-Whitney U test. (H) NREM sleep spiking
758 beta episode probability, beta episode duration and beta episode frequency, normal vs.
759 MPTP, GPe, GPi and STN, **P < 0.005, ***P < 0.0001, n.s., non-significant, Mann-
760 Whitney U test.
761

762 **Figure 3** Parkinsonism is associated with an increase in beta oscillations in the
763 cerebral cortex during NREM sleep. (A) Examples of central EEG (C1) activity during
764 normal NREM sleep (top, notice the predominant slow oscillatory activity), and
765 during Parkinsonian NREM sleep (bottom, where beta activity is more prominent).
766 Horizontal bar, 0.5 s. Vertical bars, 50 μ V. (B) Power spectra of scalp EEG (average
767 over frontal, central and occipital electrodes ipsilateral to BG electrodes) during
768 NREM sleep and wakefulness, normal vs. MPTP nights. Pale shading represents
769 s.e.m. $n = 67$ and 19 nights for the normal and MPTP recordings, respectively. (C)
770 NREM sleep and wakefulness EEG beta power (normalized as previously) for both
771 conditions and sleep stages, $**P < 0.005$, $***P < 0.0001$, Mann-Whitney U test.
772 During MPTP, NREM beta power was not significantly different from the
773 wakefulness beta power, Wilcoxon signed rank test. (D) NREM sleep EEG beta
774 episode probability, beta episode duration (upper inset) and beta episode frequency
775 (lower inset), normal vs. MPTP, $***P < 0.0001$, Mann-Whitney U test.
776

777 **Figure 4** Beta oscillations during NREM sleep are coherent within and between the
778 BG and cerebral cortex. (A-B) Examples of field potential (FP, A) and spiking activity
779 (B) recorded simultaneously by two microelectrodes in the GPi during Parkinsonian
780 NREM sleep. Horizontal bar, 0.5 s (A) or 0.25 s (B). Vertical bars, 50 μ V. Spiking
781 traces represent 1 s. (C-D) Coherence of simultaneously recorded FP (C) and spiking
782 (D) in the BG during NREM sleep in the Parkinsonian monkey. Dashed lines represent
783 the same recording sites, with time-shifted FP/spiking traces. Pale shading represents
784 s.e.m. For FP and spiking coherence, $n = 278, 85$ and 26 paired recordings for the
785 GPe, GPi and STN, respectively. Inset, area under the curve (AUC) evaluated for the
786 beta range (10-17 Hz), the baseline being the average 20-40 Hz range coherence, non-
787 shifted (left boxes) vs. shifted data (right boxes). $***P < 0.0001$, Mann-Whitney U
788 test. (E) FP-spiking coherence for the MPTP data vs. shifted data, conventions and
789 inset as in (C) and (D). For the GPe, GPi and STN, respectively, $n = 211, 51$ and 43
790 recordings. (F) Coherence between ipsilateral EEG electrodes during Parkinsonian
791 NREM sleep, relative to shifted data ($n = 19$ nights). Inset, AUC as before. $**P <$
792 0.005 , $***P < 0.0001$, Mann-Whitney U test. (G-H) Coherence between averaged
793 ipsilateral EEG and BG FP (G) or spiking (H) activity during Parkinsonian NREM
794 sleep. Dashed lines represent the coherence spectra between shifted data. Insets, AUC
795 for the non-shifted and shifted data, as previously.

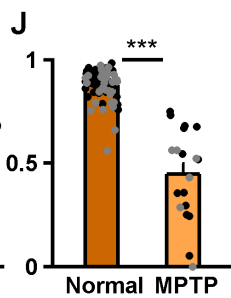
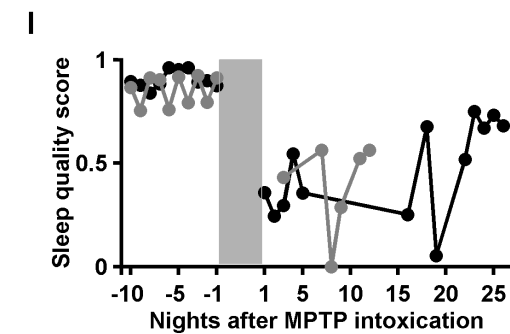
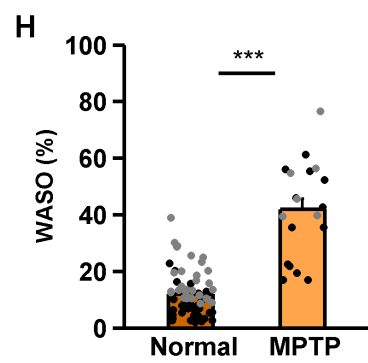
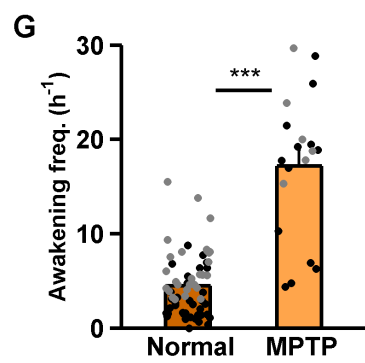
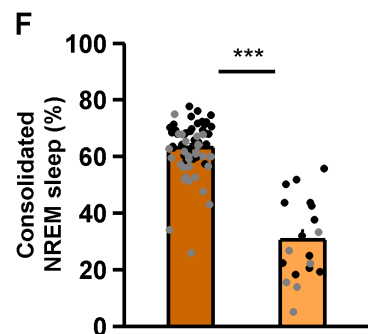
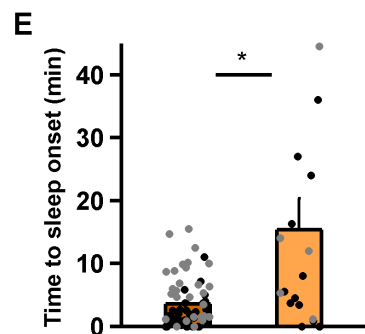
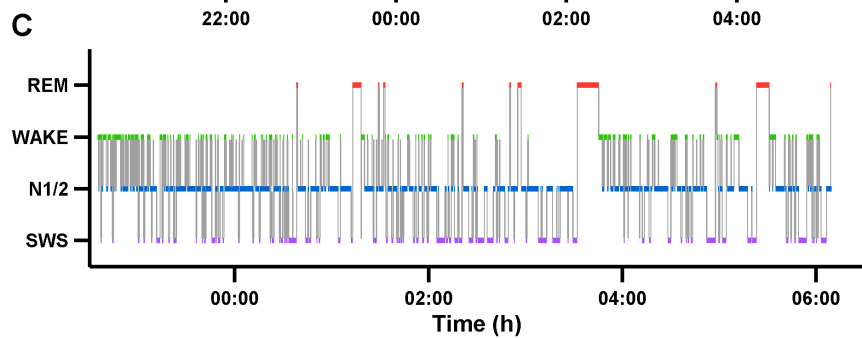
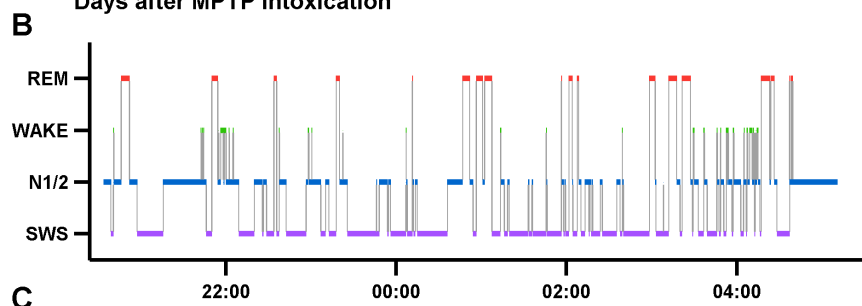
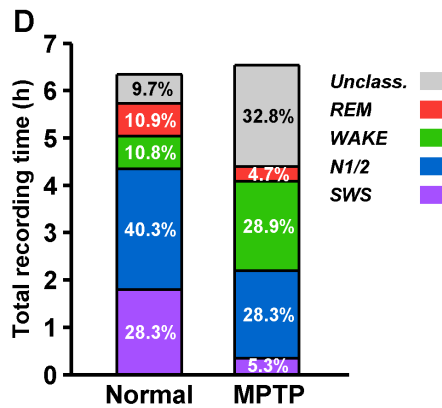
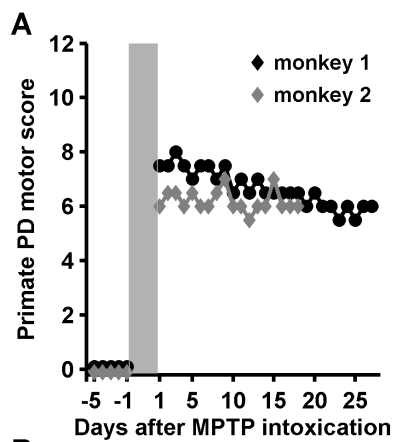
796 **Figure 5** The increase in beta activity in the BG is correlated with a decrease in BG
797 and cortical slow oscillatory activity. (A) Power spectra of firing rates recorded during
798 NREM sleep in the normal (dark traces) and MPTP monkey (light traces), GPe (red),
799 GPi (blue) and STN (green). Error bars represent s.e.m. Normal, n = 305, 172 and 94
800 neurons for GPe, GPi and STN, respectively. MPTP, n = 211, 51 and 43 for GPe, GPi
801 and STN, respectively. (B) Average NREM sleep firing rate 0.1-1 Hz relative power,
802 for each BG nucleus, across recording nights, normal vs. MPTP monkey. *P < 0.05,
803 ***P < 0.0001, Mann-Whitney U test. (C) Bilateral frontal, central and occipital EEG
804 power spectra in the normal (dark trace, n = 67 nights) and MPTP monkey (light trace,
805 n = 19 nights). (D) Average EEG slow oscillation (SO, 0.1-2 Hz) relative power
806 during NREM sleep, across recording nights, normal vs. MPTP monkey. *P < 0.05,
807 Mann-Whitney U test. (E-F) Firing rate slow oscillation power for the different nuclei
808 of the BG, divided into four quartiles by the degree of FP (E) or spiking (F) beta
809 power recorded by the same electrode in the same neuronal site. As beta activity
810 became stronger, firing rate slow oscillatory activity decreased. Colored traces
811 represent recording sites from the GPe (red), GPi (blue) and STN (green). Purple bars
812 represent the average across all recording nights from all BG nuclei. Error bars
813 represent s.e.m. (G) Example scatter plots depicting the correlation between BG FP
814 beta power and EEG SO power during NREM sleep following MPTP intoxication,
815 GPe (red), GPi (blue) and STN (green). Each point represents one 10 s NREM sleep
816 epoch. (H) Average Pearson's correlation coefficients between BG FP beta power and
817 EEG SO activity, for all the sites and units exhibiting a significant correlation with the
818 EEG SO (white, percent out of all sites and units exhibiting beta activity), n = 72, 28
819 and 8 sites for GPe, GPi and STN, respectively. A single point in the STN bar (at 0.53)
820 is not included in this plot. (I) Same as (G), only for the correlation between BG

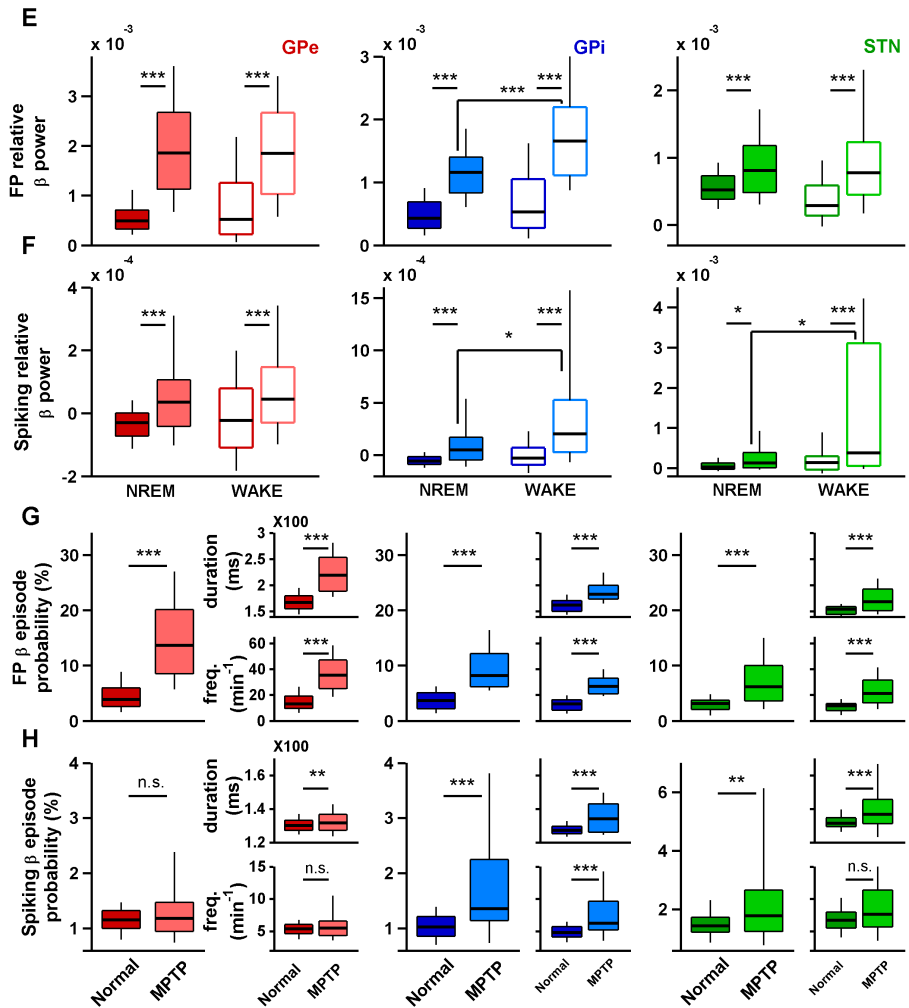
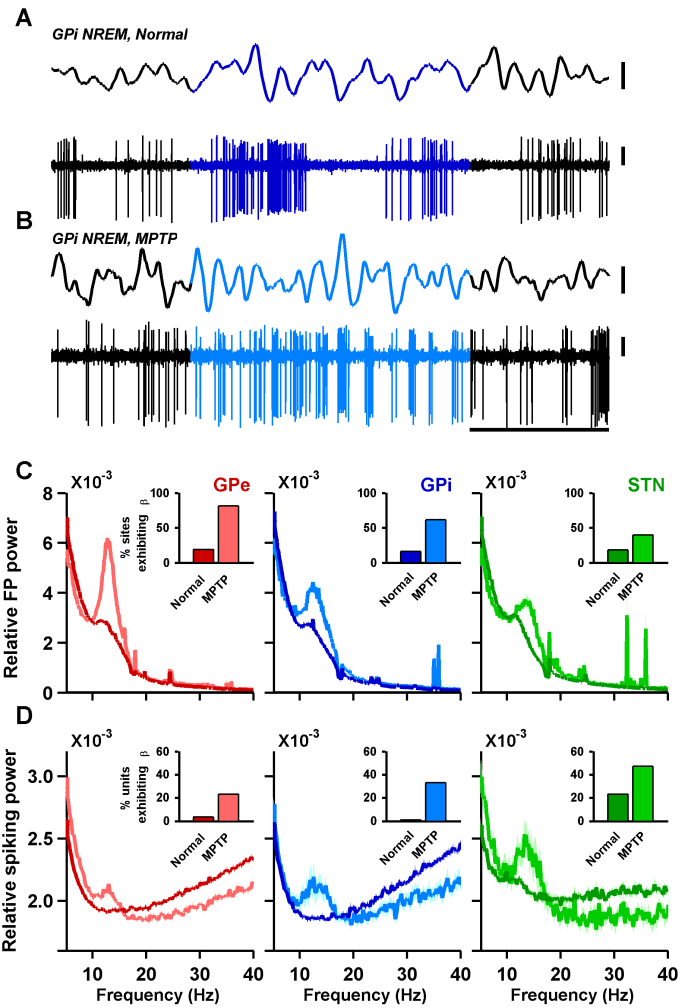
821 spiking beta power and EEG SO power. (J) Same as (H), only for Pearson's correlation
822 coefficients between BG spiking beta power and EEG SO activity. $n = 11, 5$ and 2
823 sites.

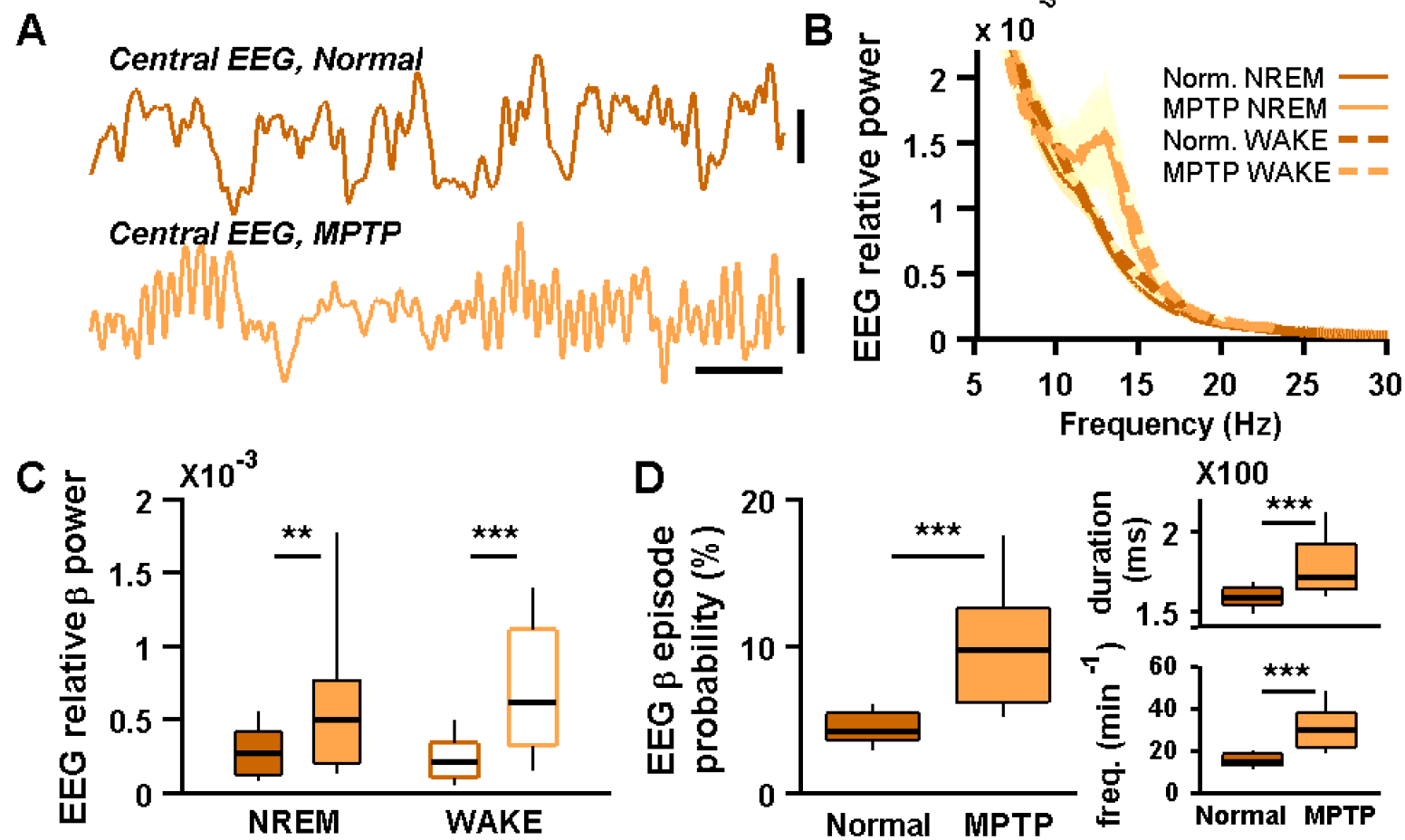
824 **Figure 6** BG beta activity rises before spontaneous awakening and correlates with the
825 severity of insomnia in Parkinsonism. (A) FP beta power in the GPe (red), GPi (blue)
826 and STN (green) during NREM sleep decreases as sleep deepens, is relatively low
827 during SWS, and increases steadily before awakening (dashed red line), when it
828 plateaus. Shading represents s.e.m. Numbers of recording sites as in Fig. 2. SWS beta
829 power was lower than the beta power in the first NREM epoch after falling asleep for
830 GPe and STN, lower than the average N1/2 beta power (all BG structures), and lower
831 than the beta power 10 s before wake-up, for GPe. For STN, the beta power 40 s after
832 falling asleep was lower than 10 s before wake-up. For all structures, the beta power
833 was not significantly different for any one of the wakefulness points, Kruskal-Wallis
834 H test, $P > 0.05$. For all structures, the average post-awakening beta power was greater
835 than the beta power during SWS and greater than the beta power 40 s after falling
836 asleep. Unless stated otherwise, the statistical test used for all comparisons was the
837 Mann-Whitney U test, and all $P < 0.05$. (B) Same as (A), only for FP beta episode
838 probability. All statistical relationships in (A) also hold for the beta probability, except
839 for the relationship between the first NREM sleep epoch and SWS, which was true for
840 GPe and GPi, and the N1/2 vs. SWS comparison, which was not significant for STN.
841 (C) Same as (A-B), only for FP-EEG beta range coherence. In the GPe, SWS beta
842 coherence was lower than beta coherence for the first NREM epoch, lower than beta
843 coherence for the average of the last three epochs before awakening and lower than
844 N1/2 beta coherence. In the STN, the beta coherence 10 s before awakening was
845 greater than the SWS beta coherence. For all structures, the beta coherence was not
846 significantly different for any one of the wakefulness points, Kruskal-Wallis H test, P
847 > 0.05 . For GPi, the average post-awakening beta coherence was greater than during
848 SWS and 40 s before awakening. (D) EEG SO power during NREM sleep increases as

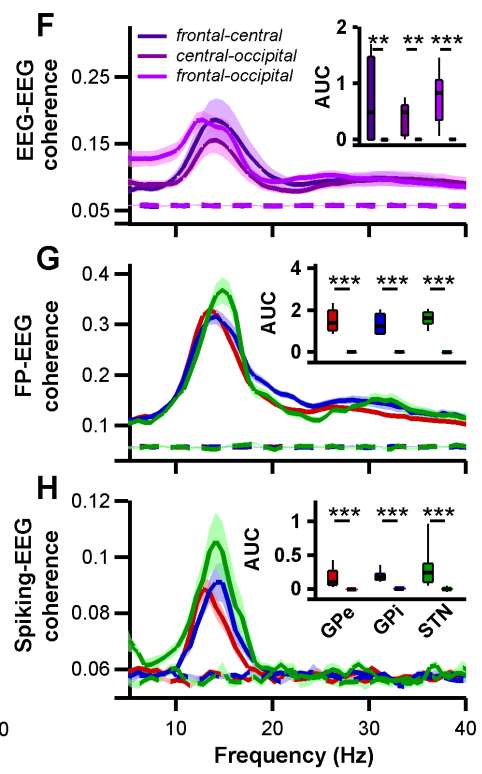
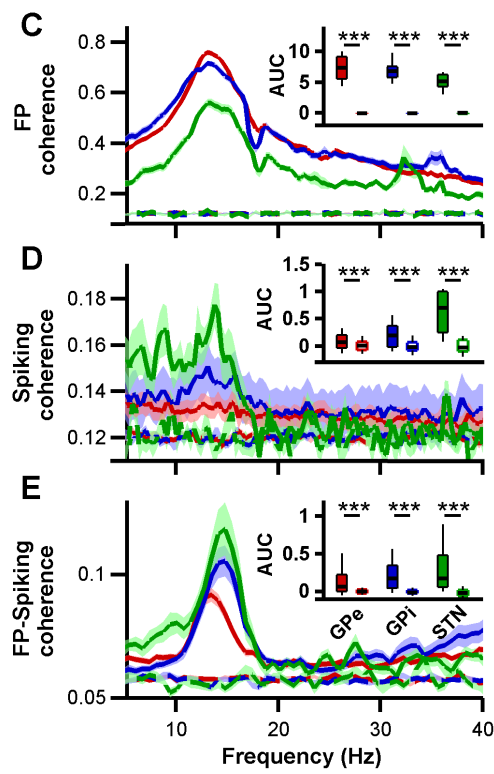
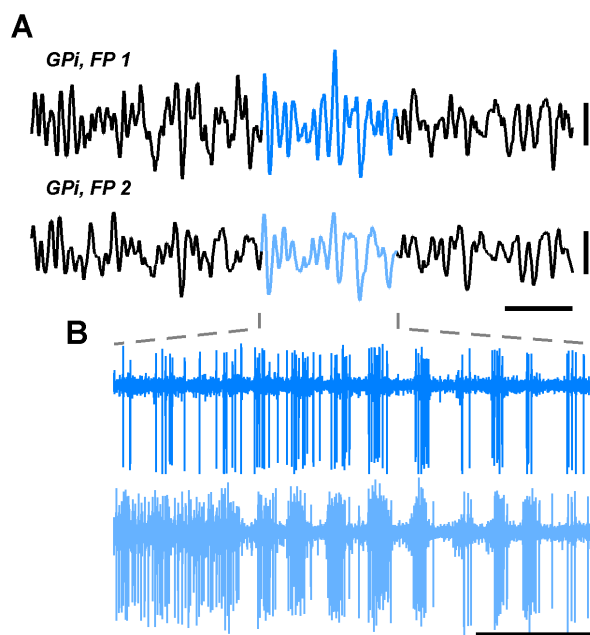
849 sleep deepens, is relatively high during SWS and before awakening, and decreases
850 abruptly after awakening, when it plateaus. SWS SO power was greater than SO
851 power in the first NREM epoch after falling asleep, N1/2 SO power and post-
852 awakening SO power. EEG SO power was not significantly different for any of the 40
853 s to 10 s points before awakening, and was not significantly different for any one of
854 the wakefulness points, Kruskal-Wallis H test, $P > 0.05$. Finally, the average EEG SO
855 power 20 s and 30 s after awakening was significantly lower than the average EEG SO
856 power 40 s to 10 s before awakening.

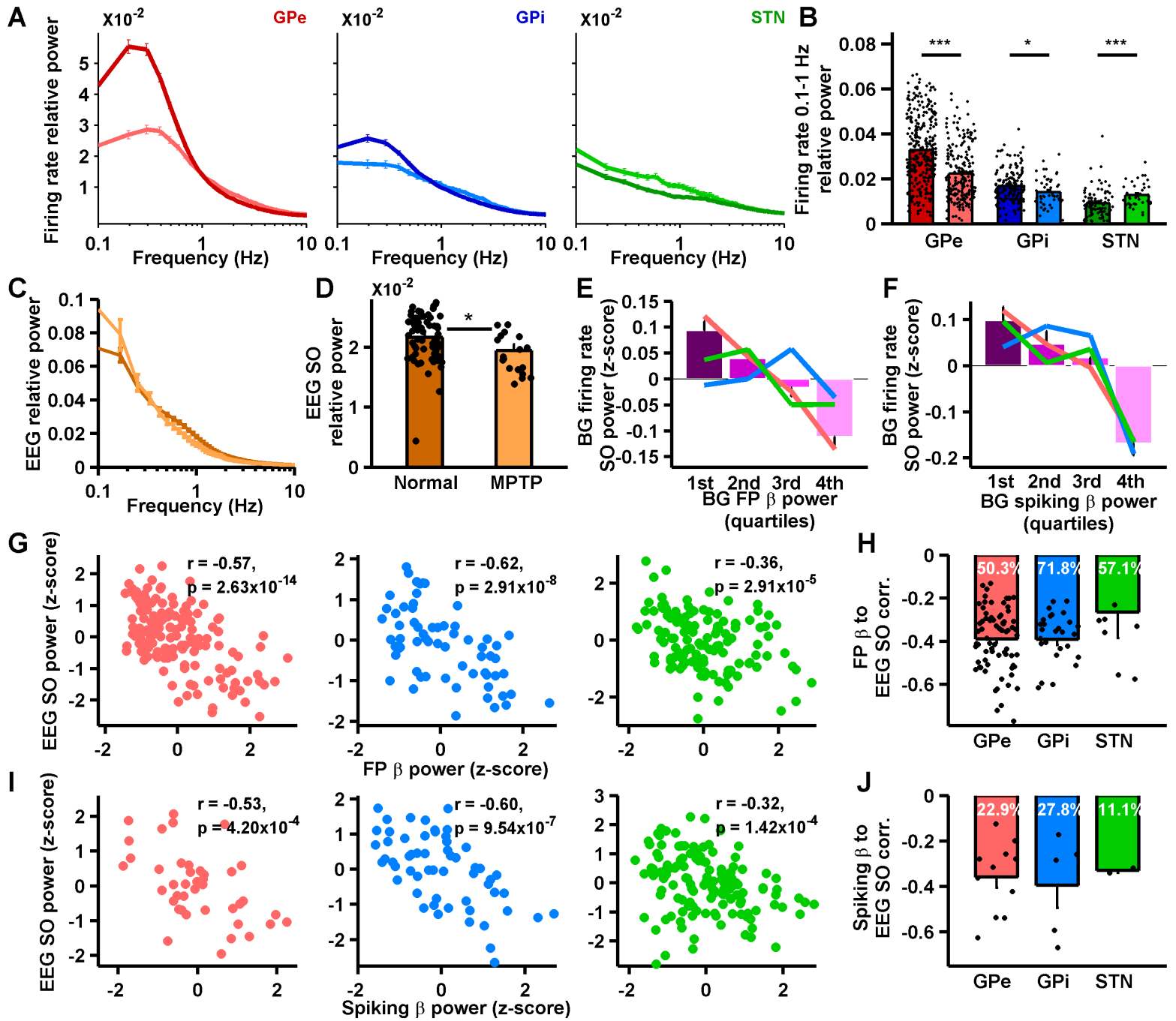
857 (E) Increased FP NREM sleep beta power in the BG correlates with poorer sleep. Left,
858 NREM sleep (% out of all classified epochs), middle, wakefulness (%), right, hourly
859 awakening frequency. Shading represents s.e.m. Beta power levels are shown on the x
860 axis as sixths of the total beta range recorded for each night, to enable comparisons
861 between nights. Lowest vs. highest normalized beta power group, for the MPTP
862 monkey, NREM sleep percentage was lower for the highest beta group, and both
863 wakefulness percentage and awakening frequency were higher for the highest beta
864 group, for all structures except wakefulness percentage for STN ($P < 0.05$, Mann-
865 Whitney U test). (F) Same as (E), only for spiking beta power. Lowest vs. highest
866 normalized beta power group, for the MPTP monkey, NREM sleep percentage was
867 lower for the highest beta group, and both wakefulness percentage and awakening
868 frequency were higher for the highest beta group, for GPe and STN only ($P < 0.001$,
869 Mann-Whitney U test).

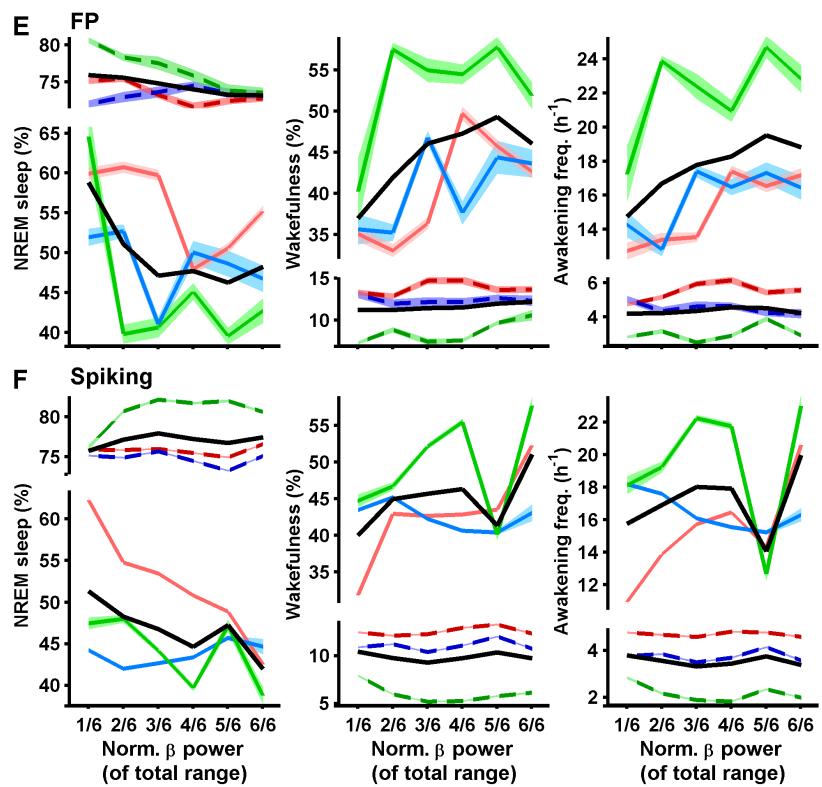
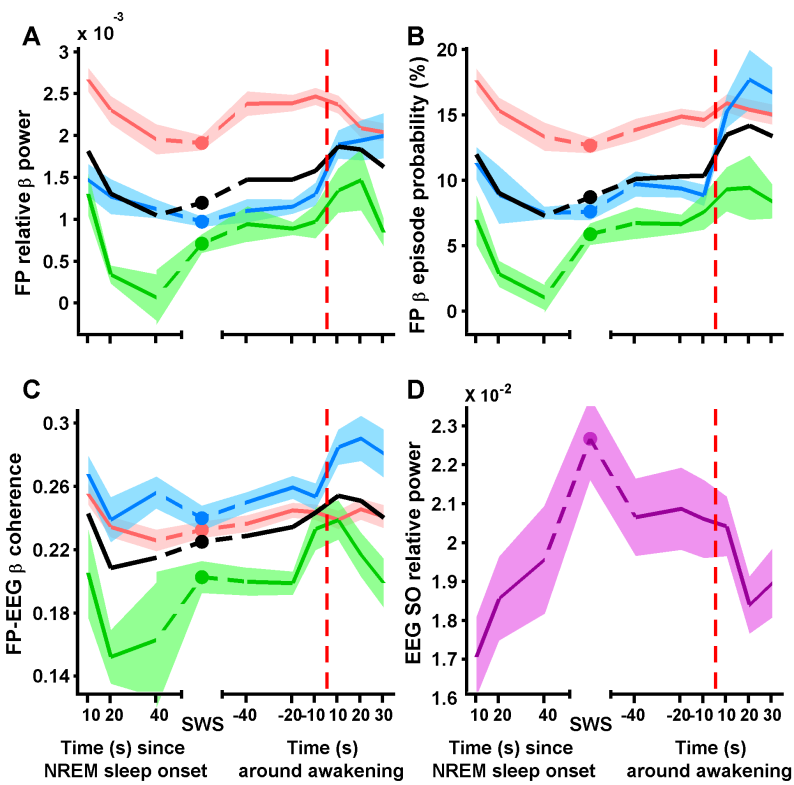












Normal: GPe - - - GPI - - - STN - - - MPTP: GPe - - - GPI - - - STN - - - Average - - -